Journal of Inclusion Phenomena and Molecular Recognition in Chemistry **31:** 1–16, 1998.

Diverse Modes of Solvent Inclusion in Crystalline Pseudopolymorphs of the Anthelmintic Drug Niclosamide

M. R. CAIRA*
Department of Chemistry, University of Cape Town, Rondebosch, 7700, South Africa

E. C. VAN TONDER, M. M. DE VILLIERS and A. P. LÖTTER
Research Institute for Industrial Pharmacy, Potchefstroom, University for CHE, Potchefstroom 2520, South Africa

(Received: 4 October 1996; in final form: 28 October 1997)

Abstract. Single crystal X-ray structures of solvated forms of the anthelmintic drug Niclosamide reveal distinctly different modes of inclusion for different solvents. These modes are, respectively, cavity occupation by water molecules in 1 : 1 niclosamide·H_2O, channel occupation by tetrahydrofuran molecules in 1 : 1 niclosamide·THF, and intercalation by tetraethylene glycol molecules in 2 : 1 niclosamide·TEG. In all three compounds the host drug molecule adopts the same, nearly planar conformation, which is maintained by an intramolecular N—H···O hydrogen bond. Host-guest recognition invariably involves hydrogen bonding between the drug hydroxyl group and an oxygen acceptor atom of the solvent molecule. The observed modes of solvent inclusion can be reconciled with the behaviour of the crystals on heating.

Keywords: drug pseudopolymorphs, drug solvates, anthelmintic, Niclosamide, solvent inclusion.

1. Introduction

Inclusion of solvents during crystallisation of drug molecules, whether accidental or by design, has important consequences in the pharmaceutical industry [1]. Drug solvates, or 'pseudopolymorphs', generally have crystal structures which differ from that of the unsolvated drug and consequently possess different properties, including solubility, and physical or chemical stability. These solvates may also exhibit structural features typical of clathrates and we have described such cases previously [2, 3]. Frequently, drug host and solvent guest associate in the crystal solvate by hydrogen bonding and the term 'coordinato-clathrate' is an appropriate designation [4]. Here we describe a series of drug solvates in which host-guest recognition is based on (drug) O—H···O (solvent) hydrogen bonding. The title drug, niclosamide: [5-chloro-*N*-(2-chloro-4-nitrophenyl)-2-hydroxybenzamide], shown in Figure 1, is a salicylamide derivative which has for many years been the drug of choice in the treatment of most tapeworm infections [5]. It is reported to exist as pale

* Author for correspondence.

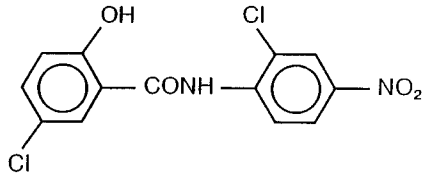

Figure 1. Structure of Niclosamide.

yellow crystals (m.p. 225–230 °C) which are practically insoluble in water [6]. During a comprehensive study of the drug [7], aimed at isolating different polymorphic and pseudopolymorphic forms which may be suitable for pharmaceutical formulations, single crystals of three solvated forms were obtained. These species, niclosamide·H_2O (**1**), niclosamide·THF (**2**) and (niclosamide)$_2$·TEG (**3**), grown from wet acetone, tetrahydrofuran (THF) and tetraethylene glycol (TEG), respectively, were characterised by hot stage and scanning electron microscopy, infrared spectroscopy, thermal analysis and powder X-ray diffraction. Here we report their single crystal X-ray structures which reveal that, while the conformation of the host drug molecule in the three inclusion compounds is invariant, the solvent molecules H_2O, THF and TEG are included in distinctly different modes. These modes of inclusion are consistent with thermogravimetric (TG) and differential scanning calorimetric (DSC) data for these species. The detailed TG and DSC data for these compounds will shortly be published elsewhere as part of a more general physicochemical characterisation of niclosamide [8]. The structure of (niclosamide)$_2$·TEG is of particular interest as this is, to our knowledge, the first crystal structure of an inclusion compound containing the TEG molecule as a guest.

2. Experimental

Details of crystal preparation and preliminary physicochemical characterisation are reported elsewhere [8]. X-ray precession photography was used to determine crystal symmetries and space groups. For **2**, the conditions limiting observed reflections were consistent with the orthorhombic space groups $Pnma$ (No. 62) or $Pn2_1a$ (alternative setting of $Pna2_1$, No. 33). Intensity data were collected on an Enraf-Nonius CAD4 diffractometer using Mo$K\alpha$ radiation (λ = 0.7107 Å) and scan modes ω–2θ for **1** and **2**, and ω for **3**. Variable scan speeds were used depending on I and $\sigma(I)$ with a maximum time of 40 s per reflection. A variable scan width ω of (0.80 + 0.35 tan θ)° was used for **1** and **2**; for **3**, ω was (0.75 + 0.35 tan θ)°. The variable aperture width was (1.12 + 1.05 tan θ) mm in all cases. Crystals of **1** were stable in air and no special precautions were necessary. Compound **2** desolvated within minutes of exposure to air and the crystal was therefore mounted in mother liquor in a Lindemann capillary for data collection. Compound **3** showed very slow decomposition in air but the crystal was nevertheless treated similarly to **2** to minimise solvent loss. Crystals of **2** and **3** were moderately cooled to enhance

intensity data quality. Accurate unit cell parameters were obtained by least-squares analysis of angular data between 16° and 17°θ. During data collection, crystal stability was monitored by hourly measurement of three reference reflection intensities and orientation control was performed every 200 measured reflections. For **2**, there was an overall increase in the standard intensities indicating crystal growth in mother liquor during data collection. However, this growth was anisotropic (3.0, 10.8 and 5.0% intensity increases for the individual standard reflections) and scaling of the data based on these standards was therefore not feasible. The observed standard intensity increase was regarded as far less serious for the purposes of this analysis than the significant intensity decreases (>20%) due to crystal desolvation occasioned in earlier data collection attempts. All intensity data were corrected for Lorentz-polarization effects as well as for absorption.

The structures of **1** and **3** were solved using program SHELX-86 [9] and refined routinely with program SHELX-76 [10] using full-matrix and blocked full-matrix routines, respectively. H atoms were located in difference electron density maps but were generally placed in idealised riding positions with C—H 1.00 Å. H atoms of the water molecule in **1** were constrained at 1.0 Å from their parent O atom while the host hydroxyl H atom refined freely. H atoms in **3** were treated analogously. In the final refinements, non-H atoms refined anisotropically and H atoms isotropically.

Structure solution and refinement of **2** were complicated by the space group ambiguity. Although intensity statistics indicated centrosymmetry, the best direct methods solution in the centrosymmetric space group had a figure of merit of 0.11 and revealed only 18 of the host non-hydrogen atoms whereas that in the non-centric space group $Pn2_1a$ had a figure of merit of 0.025 and revealed all of the host atoms. Refinement of **2** was performed in both space groups, $Pnma$ requiring all host atoms to be located in a crystallographic mirror plane and the guest THF molecule to be disordered across the mirror plane, whereas no constraints were placed on either host or guest in $Pn2_1a$. Furthermore, difference electron density maps phased on the host molecule in space group $Pn2_1a$ revealed the guest molecule (including H atoms) unequivocally, with no evidence of disorder. Consideration of final refined host bond lengths and angles as well as R-factors was not decisive in assigning the space group. Intensity statistics biased towards centrosymmetry can result from a nearly centric arrangement of molecules, as in the present case [11]. The solution in the non-centric space group was eventually accepted as correct on the strength of the history of the behaviours of the two models. The model in $Pn2_1a$ had the additional merit that the niclosamide molecule could show deviations from strict planarity, consistent with what was observed in three other instances in this study (one crystallographically independent drug molecule in **1** and two independent drug molecules in **3**, all located in general crystallographic positions). In the final refinement of **2**, non-H atoms refined anisotropically and H atoms refined isotropically in idealised riding positions except for the host hydroxyl H atom which refined freely. The C—C and C—O distances in the THF molecule were constrained to values observed previously [2]. In view of

the increase in average intensity observed, no attempt was made to determine the absolute structure of the crystal of **2**. Refinement in all cases involved minimisation of $\Sigma w(|F_0| - |kF_c|)^2$ with weights w of the form $[\sigma^2(F_0) + gF_0^2]^{-1}$ optimised to yield constant distributions of $\Sigma(w\Delta F)^2$ with $\sin\theta$ and $(F_0/F_{0,\max})^{1/2}$. Molecular parameters were calculated with program PARST [12] and molecular drawings were made with PLUTO [13]. The topology of guest inclusion was studied using the program MOLMAP [14].

3. Results and Discussion

Table I lists crystal data and details of crystallographic refinements for **1**, **2** and **3**. The compound stoichiometries were deduced from routine thermogravimetry [7]. Final atomic coordinates and isotropic thermal parameters ($U_{\text{eq}} = (1/3)\Sigma_i\Sigma_j U_{ij} a_i^* a_j^* a_i \cdot a_j$) for non-H atoms are listed in Tables II–IV. Primary intramolecular and intermolecular hydrogen bonds in **1**–**3** are listed in Table V.

3.1. STRUCTURE OF NICLOSAMIDE · H_2O (**1**)

Figure 2 shows the asymmetric unit of the monohydrate **1** with atomic numbering. The drug molecule is locked into a nearly planar conformation which is stabilised primarily by an intramolecular hydrogen bond N(11)—H(11)···O(20) (Table V). The coplanarity of the phenyl rings may be attributed to additional cohesive, but weaker, intramolecular hydrogen bonds, C(6)—H(6)···O(13) and Cl(7)···H(11)—N(11). Kosheleva and Bekhli [15] studied niclosamide conformations by IR spectroscopy and identified two planar conformations, α and β, which differ in their intramolecular hydrogen bonding arrangements. In the α-conformer, the intramolecular hydrogen bond links the carbonyl and hydroxyl groups (C=O···H—O), whereas in the β-conformer, the hydrogen bond links the N—H group and the hydroxyl group (N—H···O—H). The conformation observed in **1** thus corresponds to the β-conformation. Kosheleva and Bekhli concluded that the intramolecular hydrogen bond in the niclosamide polymorph containing the β-conformer is weaker than that occurring in the α-polymorph [15], leading to thermolabile transformation of the β-polymorph to the 'stable α-polymorph'. We have, however, encountered only the β-conformer of niclosamide in this study of its solvated forms.

Each of the phenyl rings in **1** is planar to within 0.006 Å and the dihedral angle between them is 9.8(1)°. The slightly concave shape of the molecule is associated with non-zero torsion angles C(6)—C(1)—N(11)—C(12), −7.1(4)°, and C(1)—N(11)—C(12)—O(13), −2.9(4)°. Bond lengths and bond angles are in the expected ranges and do not warrant discussion. Atom O(22) of the included water molecule is an acceptor in a nearly linear hydrogen bond O(20)—H(20)···O(22), which involves the drug hydroxyl group. The short O(20)···O(22) distance indicates strong host-guest interaction. The H atoms of the water molecule engage in

Table I. Crystal data and experimental details for compounds **1–3**.

	1	**2**	**3**
Compound[a]	$H{\cdot}H_2O$	$H{\cdot}C_4H_8O$	$H_2{\cdot}C_8H_{18}O_5$
M/g mol^{-1}	345.14	399.23	848.47
a/Å	11.332 (2)	11.313 (3)	7.888 (3)
b/Å	16.964 (2)	6.805 (2)	37.56 (1)
c/Å	7.346 (3)	22.993 (8)	12.630 (6)
$\alpha/^\circ$	90.0	90.0	90.0
$\beta/^\circ$	98.28 (2)	90.0	90.78 (4)
$\gamma/^\circ$	90.0	90.0	90.0
V/Å^3	1397.5 (7)	1770.1 (9)	3742 (3)
Z	4	4	4
Crystal system	Monoclinic	Orthorhombic	Monoclinic
Space group	$P2_1/c$	$Pn2_1a$	$P2_1/c$
μ(MoK_α/mm^{-1})	0.488	0.396	0.384
F(000)	704	824	1752
D_c/g cm^{-3}	1.641	1.498	1.506
Crystal size/mm	0.22 × 0.25 × 0.34	0.50 × 0.50 × 0.50	0.30 × 0.30 × 0.50
Temperature/K	294	252	256
Scan range/θ°	1–25	1–25	1–25
Index range	±13, 20, 8	13, 8, 27	±9, 44, 15
Intensity variation/%	−2.4	+6.2	−1.3
Absorption corr. range	0.9699–0.9994	0.9318–0.9983	0.9838–0.9993
Data measured	2758	1839	7013
Unique data	2303	1532	5304
Observed data	2079	1287	3942
n in $I > n\sigma(I)$	2	2	1
R_{int}	0.015	0.043	0.028
Parameters	213	239	515
Average Δ/σ	0.001	0.50	0.01
R	0.032	0.057	0.045
R_{W}	0.032	0.066	0.037
g in weights w	0.000	0.002	0.000
S	2.755	1.691	1.964
$\Delta\rho$/eÅ^{-3}, max	0.21	0.38	0.29
$\Delta\rho$/eÅ^{-3}, min	−0.30	−0.36	−0.25

[a] H = host molecule $C_{13}H_8Cl_2N_2O_4$.

hydrogen bonds to O atoms of symmetry related host drug molecules as shown in Figure 3, a stereodiagram of the crystal packing viewed down the shortest cell axis. Water molecules clearly play a crucial role in maintaining the crystal structure. The hydrogen bonds in which water H atoms are donors are listed in Table V and

Table II. Fractional atomic coordinates ($\times 10^4$) and equivalent isotropic displacement parameters (Å$^2 \times 10^3$) for non-hydrogen atoms in **1**.

Atom	x/a	y/b	z/c	U_{eq}
C(1)	7342 (2)	6197 (1)	3142 (3)	30 (1)
C(2)	8336 (2)	6553 (1)	2526 (3)	30 (1)
C(3)	9319 (2)	6118 (1)	2234 (3)	34 (1)
C(4)	9309 (2)	5321 (1)	2576 (3)	35 (1)
C(5)	8354 (2)	4947 (1)	3172 (4)	37 (1)
C(6)	7363 (2)	5384 (1)	3444 (4)	36 (1)
Cl(7)	8366 (0)	7559 (0)	2176 (1)	39 (0)
N(8)	10362 (2)	4860 (1)	2305 (3)	43 (1)
O(9)	10364 (2)	4159 (1)	2588 (4)	73 (1)
O(10)	11209 (2)	5210 (1)	1807 (3)	60 (1)
N(11)	6408 (1)	6694 (1)	3433 (3)	32 (1)
C(12)	5320 (2)	6496 (1)	3870 (3)	31 (1)
O(13)	4992 (1)	5813 (1)	4004 (3)	48 (1)
C(14)	4518 (2)	7170 (1)	4172 (3)	29 (1)
C(15)	3391 (2)	6962 (1)	4580 (3)	32 (1)
C(16)	2583 (2)	7532 (1)	4889 (3)	33 (1)
C(17)	2861 (2)	8324 (1)	4803 (3)	38 (1)
C(18)	3960 (2)	8541 (1)	4382 (3)	36 (1)
C(19)	4794 (2)	7971 (1)	4063 (3)	32 (1)
O(20)	5875 (1)	8186 (1)	3651 (3)	43 (1)
Cl(21)	1187 (0)	7255 (0)	5389 (1)	44 (0)
O(22)	6338 (2)	9678 (1)	3294 (3)	55 (1)

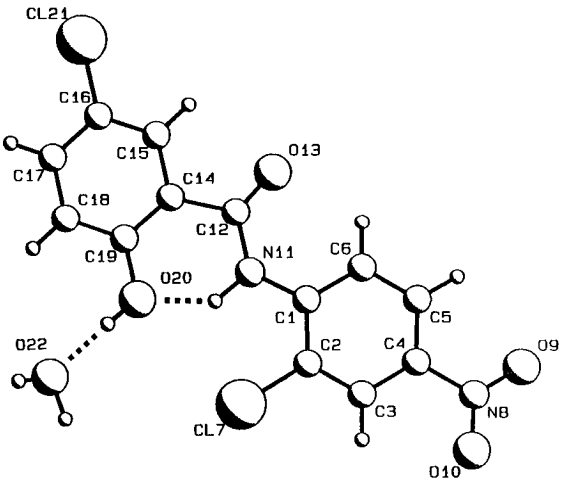

Figure 2. Structure, conformation and atomic numbering of the asymmetric unit in **1**. Principal hydrogen bonds are shown as dotted lines.

Table III. Fractional atomic coordinates ($\times 10^4$) and equivalent isotropic displacement parameters (Å^2 $\times$ 10^3) for non-hydrogen atoms in **2**.

Atom	x/a	y/b	z/c	U_{eq}
C(1)	−230 (4)	1738 (21)	5896 (2)	39 (2)
C(2)	858 (4)	1734 (19)	6195 (2)	39 (1)
C(3)	925 (4)	1733 (20)	6789 (2)	44 (2)
C(4)	−110 (5)	1795 (19)	7097 (2)	43 (2)
C(5)	−1192 (4)	1641 (20)	6831 (2)	44 (2)
C(6)	−1272 (5)	1873 (19)	6243 (3)	41 (2)
Cl(7)	2156 (1)	1741[a]	5797 (1)	49 (0)
N(8)	−41 (4)	1735 (20)	7731 (2)	59 (2)
O(9)	921 (4)	1757 (24)	7963 (2)	109 (3)
O(10)	−944 (4)	1762 (23)	8011 (2)	90 (2)
N(11)	−220 (3)	1711 (16)	5298 (2)	42 (1)
C(12)	−1172 (4)	1676 (19)	4921 (2)	42 (2)
O(13)	−2191 (3)	1780 (18)	5088 (2)	59 (2)
C(14)	−860 (4)	1733 (20)	4292 (2)	44 (2)
C(15)	−1843 (5)	1773 (21)	3917 (2)	47 (2)
C(16)	−1681 (5)	1751 (22)	3326 (2)	54 (2)
C(17)	−541 (6)	1645 (18)	3088 (2)	52 (2)
C(18)	420 (5)	1731 (23)	3450 (2)	52 (2)
C(19)	252 (5)	1715 (22)	4051 (2)	45 (2)
O(20)	1217 (3)	1717 (17)	4409 (2)	61 (2)
Cl(21)	−2885 (1)	1728 (11)	2866 (1)	98 (1)
O(22)	3240 (5)	1077 (12)	3912 (3)	90 (4)
C(23)	4135 (12)	38 (17)	4221 (8)	117 (6)
C(24)	4715 (8)	1621 (23)	4559 (4)	127 (6)
C(25)	4589 (22)	3353 (23)	4178 (7)	191 (12)
C(26)	3789 (9)	2791 (16)	3697 (5)	102 (5)

[a] Fixed coordinate to define the origin in the polar space group.

involve a nitro-group O acceptor atom for one H atom of the water molecule, and a carbonyl O acceptor atom for the other.

The differential scanning calorimetric (DSC) trace for **1** [7] showed two separate dehydration steps at unusually high temperatures of 173 $\pm$ 5 °C and 201 $\pm$ 5 °C, implying that the water molecules are very tightly bound and that partial water loss at the lower temperature is followed by crystal rearrangement to an intermediate phase which dehydrates completely at the higher temperature. To rationalise the tight binding of water in **1**, the topology of inclusion was examined with program MOLMAP [14]. This generates plots of sections through the unit cell in which atoms are drawn with their van der Waals radii, thus allowing visualisation of the fit of guest molecules in the environment provided by the host molecules. A section of

Table IV. Fractional atomic coordinates ($\times 10^4$) and equivalent isotropic displacement parameters (Å$^2 \times 10^3$) for non-hydrogen atoms in **3**.

Atom	x/a	y/b	z/c	U_{eq}
C(1)	675 (3)	2508 (1)	12176 (2)	32 (1)
C(2)	206 (4)	2831 (1)	12653 (2)	37 (1)
C(3)	−669 (4)	2839 (1)	13587 (2)	39 (1)
C(4)	−1118 (4)	2524 (1)	14050 (2)	38 (1)
C(5)	−726 (4)	2202 (1)	13600 (2)	42 (1)
C(6)	164 (4)	2194 (1)	12670 (2)	39 (1)
Cl(7)	751 (1)	3229 (0)	12061 (1)	55 (0)
N(8)	−2039 (3)	2533 (1)	15048 (2)	44 (1)
O(9)	−2361 (3)	2822 (1)	15437 (2)	64 (1)
O(10)	−2431 (3)	2248 (1)	15447 (2)	64 (1)
N(11)	1596 (3)	2520 (1)	11245 (2)	33 (1)
C(12)	2288 (4)	2238 (1)	10710 (3)	38 (1)
O(13)	2104 (3)	1932 (1)	10987 (2)	57 (1)
C(14)	3265 (4)	2325 (1)	9742 (2)	35 (1)
C(15)	3863 (4)	2031 (1)	9187 (2)	40 (1)
C(16)	4792 (4)	2074 (1)	8285 (3)	47 (1)
C(17)	5137 (4)	2407 (1)	7893 (3)	50 (1)
C(18)	4546 (4)	2700 (1)	8426 (3)	46 (1)
C(19)	3635 (4)	2664 (1)	9354 (3)	39 (1)
O(20)	3072 (3)	2954 (1)	9885 (2)	52 (1)
Cl(21)	5578 (1)	1699 (0)	7649 (1)	71 (0)
C(22)	5190 (4)	5022 (1)	2698 (2)	36 (1)
C(23)	4709 (4)	4696 (1)	2245 (3)	40 (1)
C(24)	3738 (4)	4681 (1)	1333 (3)	48 (1)
C(25)	3248 (4)	4996 (1)	861 (3)	45 (1)
C(26)	3695 (4)	5319 (1)	1280 (2)	45 (1)
C(27)	4661 (4)	5333 (1)	2195 (3)	43 (1)
Cl(28)	5323 (1)	4300 (0)	2839 (1)	60 (0)
N(29)	2246 (4)	4983 (1)	−122 (2)	60 (1)
O(30)	1859 (4)	4691 (1)	−476 (2)	92 (1)
O(31)	1867 (4)	5262 (1)	−550 (2)	89 (1)
N(32)	6144 (3)	5013 (1)	3639 (2)	36 (1)
C(33)	6754 (4)	5297 (1)	4207 (2)	36 (1)
O(34)	6549 (3)	5604 (1)	3920 (2)	53 (1)
C(35)	7716 (4)	5216 (1)	5206 (2)	32 (1)
C(36)	8317 (4)	5513 (1)	5751 (3)	42 (1)
C(37)	9253 (4)	5475 (1)	6663 (3)	48 (1)
C(38)	9622 (4)	5144 (1)	7076 (3)	49 (1)
C(39)	9023 (4)	4848 (1)	6548 (3)	45 (1)
C(40)	8071 (4)	4879 (1)	5621 (2)	38 (1)
O(41)	7465 (3)	4588 (1)	5105 (2)	50 (1)
Cl(42)	9941 (1)	5855 (0)	7329 (1)	83 (0)
O(43)	5951 (3)	3725 (1)	7535 (2)	55 (1)
C(44)	5978 (4)	3522 (1)	6600 (2)	53 (1)

Table IV. Continued.

Atom	x/a	y/b	z/c	U_{eq}
C(45)	6452 (4)	3744 (1)	5654 (2)	51 (1)
O(46)	8002 (3)	3933 (0)	5825 (2)	50 (1)
C(47)	9501 (4)	3714 (1)	5856 (3)	52 (1)
C(48)	10580 (4)	3828 (1)	6778 (3)	55 (1)
O(49)	9714 (3)	3748 (1)	7733 (2)	49 (1)
C(50)	10350 (4)	3949 (1)	8600 (3)	61 (2)
C(51)	9549 (4)	3822 (1)	9591 (3)	64 (2)
O(52)	7769 (3)	3864 (1)	9481 (2)	54 (1)
C(53)	6857 (5)	3744 (1)	10372 (3)	67 (2)
C(54)	5006 (5)	3785 (1)	10134 (3)	64 (2)
O(55)	4416 (3)	3552 (1)	9327 (2)	62 (1)

Table V. Primary hydrogen bonds[a] in **1–3** (distances in Å, angles in °).

Compound	D	H	A	H···A	D···A	D—H···A	Symmetry translation of A
1	N(11)	H(11)	O(20)	1.77	2.612	139.6	x, y, z
	O(20)	H(20)	O(22)	1.76	2.606	176.3	x, y, z
	O(22)	H(221)	O(10)	1.96	2.934	164.8	$2-x, 1/2+y, 1/2-z$
	O(22)	H(222)	O(13)	1.91	2.845	155.4	$1-x, 1/2+y, 1/2-z$
2	N(11)	H(11)	O(20)	1.77	2.612	139.4	x, y, z
	O(20)	H(20)	O(22)	1.70	2.596	146.8	x, y, z
3	N(11)	H(11)	O(20)	1.83	2.649	136.8	x, y, z
	O(20)	H(20)	O(55)	1.76	2.586	170.3	x, y, z
	N(32)	H(32)	O(41)	1.83	2.648	137.2	x, y, z
	O(41)	H(41)	O(46)	1.90	2.655	167.9	x, y, z
	O(43)	H(43)	O(49)	2.04	2.977	156.4	x, y, z
	O(55)	H(55)	O(43)	1.67	2.662	171.5	x, y, z

[a] Maximum e.s.d.s in D···A distances and D—H···A angles are 0.007 Å and 3.1° respectively.

this kind at $y = 0.0$ is drawn for **1** in Figure 4. The two H_2O molecules within the unit cell, labeled 1 and 2, occupy a cavity bounded by the van der Waals envelopes of surrounding drug molecules. The cavity is separated from an identical cavity in the adjacent unit cell by what appears as a narrow constriction produced by drug molecules related by a centre of inversion at 1/2, 0, 0 and which separates water molecules labelled 1 and $2'$. A series of sections drawn parallel to the crystal ab-face show clearly that as the section at $z = 0.0$ is approached, the extent to which water molecules 1 and $2'$ become screened from each other by intervening host atoms increases, being effectively complete at $z = 0.0$ where host phenyl rings and carbonyl O atoms form a barrier. The water molecules are therefore confined in pairs to closed cavities. This, together with their involvement in strong

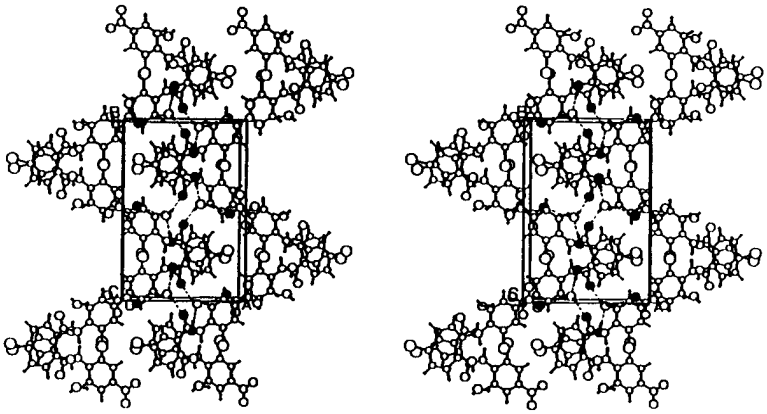

Figure 3. Stereodiagram of the crystal structure of **1**. Oxygen atoms to which H_2O molecules are hydrogen bonded are shaded for clarity.

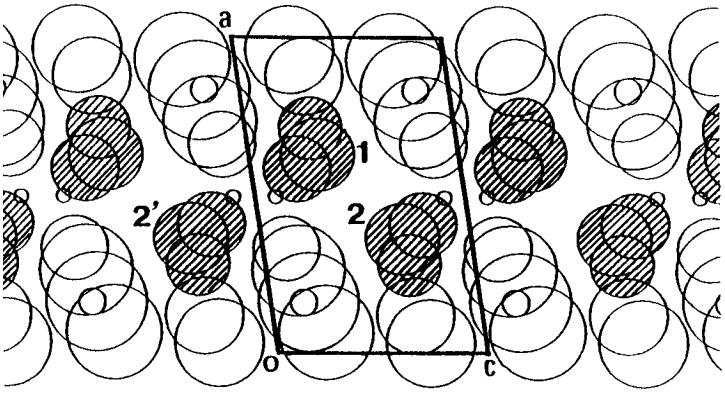

Figure 4. Section at $y = 0.0$ through the crystal of **1**. Atoms are included with their van der Waals radii and their intersections with the plane are represented by circles. Water atoms are shaded.

hydrogen bonding with surrounding drug molecules, offers an explanation for the abnormally high observed onset temperature for dehydration. The monohydrate **1** has been designated H_B [7, 8]; a second monohydrate designated H_A was also isolated but it was not possible to obtain single crystals of this form. On heating, the latter commences dehydration at 100 °C and we infer that the topology of water inclusion is quite different from that in H_B.

3.2. STRUCTURE OF NICLOSAMIDE·THF (**2**)

Figure 5 shows the asymmetric unit of **2**. It consists of one niclosamide molecule in the β-conformation [15] and one THF molecule, linked by a hydrogen bond O(20)— H(20)···O(22). The dihedral angle between the phenyl ring planes is

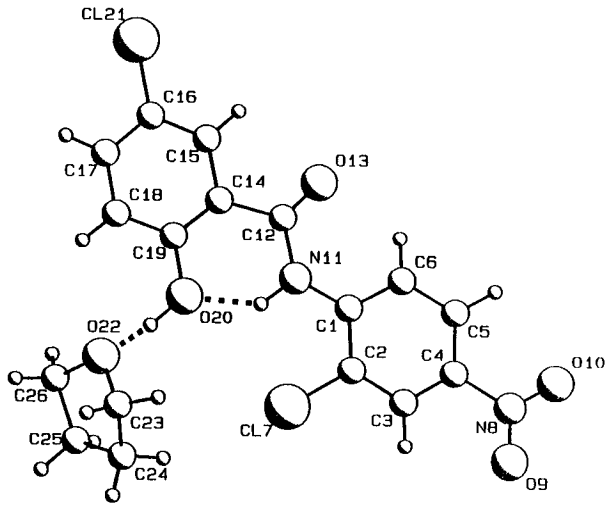

Figure 5. Structure, conformation and atomic numbering of the asymmetric unit in **2**. Principal hydrogen bonds are shown as dotted lines.

1.5(5)°. The conformation of the drug molecule is stabilised by the same set of intramolecular hydrogen bonds as observed in **1** while the conformation of the guest THF molecule is close to an envelope, with atom O(22) displaced from the plane of the four C atoms in the direction of the host hydroxyl group.

Molecular packing in the crystal is shown in the stereodiagram of Figure 6. This shows that the planes of the niclosamide molecules are nearly normal to the crystal b-axis. The operation of 2_1-axes parallel to b at the centre of each unit cell edge generates columns of closely stacked host molecules with a large cavity between them, the latter accommodating the guest THF molecules. The filling of such a cavity is shown at the centre of the unit cell in Figure 6.

Identical cavities occur at the cell corners. These are more evident in Figure 7, which shows the packing of the host molecules in space-filling representation with guest molecules omitted. Stacking of unit cells in the y-direction thus generates infinite channels occupied by guest molecules.

A characteristic feature of the crystals of **2** is their rapid desolvation on exposure to air. This occurs within minutes after removal from their mother liquor. We have previously used the difference between the onset temperature for desolvation and the boiling point of the solvent as one quantitative measure of crystal stability [16]. The instability of **2** is confirmed by thermogravimetry which yielded onset of mass loss at 30 °C [7], which is considerably lower (by 36 °C) than the normal boiling point of THF. A study of the channel topology was performed with program MOLMAP. In Figure 8, the unit cell is viewed down [100] and a section through the cell at $x = 0.5$ is shown. This gives an edge-on view of the closely stacked planes of host molecules (unshaded circles) and confirms the continuity of the

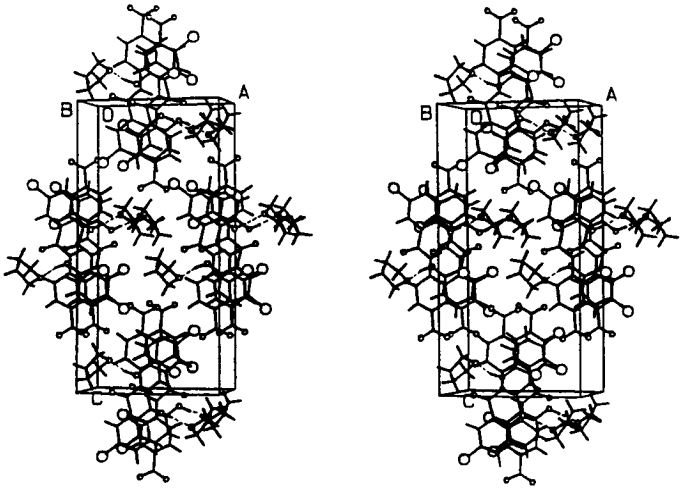

Figure 6. Stereodiagram of the molecular packing in **2**. O and Cl atoms are represented by the small and large circles, respectively.

guest-filled channel. It is very likely that such channels represent paths for facile migration of THF molecules out of the crystal and their existence is consistent with the observation of rapid crystal desolvation.

3.3. STRUCTURE OF (NICLOSAMIDE)$_2$·TEG (**3**)

The asymmetric unit of **3**, consisting of two independent host molecules (A, B) and one TEG molecule, is shown in Figure 9. Both drug molecules A and B again adopt conformations corresponding to the β-form [15], with the same intramolecular hydrogen bonds as in **1** and **2**. The dihedral angle between the phenyl rings is 2.4(1)° in molecule A and 1.8(1)° in molecule B. The A and B molecular planes are orientated differently in the crystal with a dihedral angle of 64.7(1)° between them. Figure 9 also shows the hydrogen bonding interactions within the asymmetric unit. The hydroxyl group of each niclosamide molecule donates its H atom in a hydrogen bond (O—H···O) to a guest TEG oxygen acceptor atom. For molecule A, the guest acceptor is hydroxyl atom O(55) while for B it is an ether O atom, O(46). These hydrogen bonds are strong as indicated by the short O···O distances (Table V). The guest TEG molecule adopts a folded conformation maintained by intramolecular hydrogen bonds. A 'head-to-tail' hydrogen bond O(55)—H···O(43) effectively 'cyclises' the guest and the O(43)—H···O(49) hydrogen bond acts as a 'transannular' link, leading to an 8-membered and a 10-membered ring. In documented crystal structures containing tetraethylene glycol, this molecule is usually present as a ligand coordinated to a metal ion [17]. The presence of a 'free' TEG molecule acting in a solvating role is therefore a novel feature of the structure of **3**. The molecular interactions with TEG revealed here are of interest in view

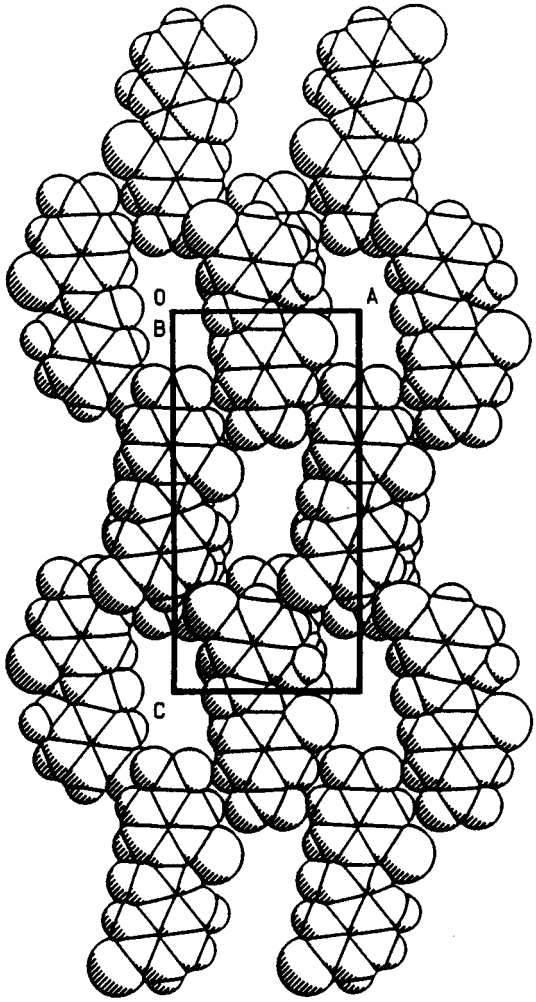

Figure 7. Space-filling representation of the packing of host molecules in **2**.

of the widespread use of PEGs, including TEG, in pharmaceutical formulations and industrial separations, both of which rely on the hydrogen bonding capacity and molecular recognition ability of these polyhydric alcohols [18]. Torsion angles for the TEG molecule are listed in Table VI. It is noted that the O—C—C—O moieties generally adopt an approximately *gauche* arrangement while the C—C—O—C moieties (with two exceptions) adopt an approximately *trans* conformation, resembling the situation in stable conformations of crown ethers (e.g. 18-crown-6).

Figure 10 is a stereodiagram of the crystal structure of **3** viewed along [001]. This shows that compound **3** may be described as an 'intercalate' since, normal to the crystal *b*-axis, infinite layers of host drug molecules alternate with layers of guest molecules. The drug molecules pack in parallel orientation within a host layer and

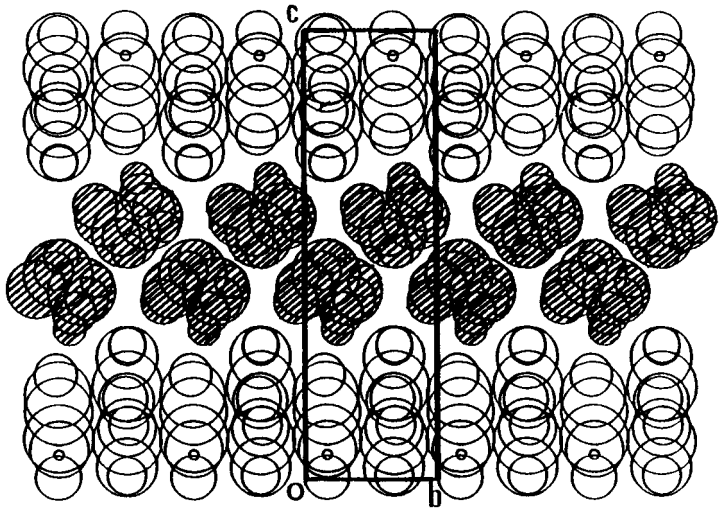

Figure 8. Section at $x = 0.5$ through the crystal of **2**. Host atoms are represented by open circles and guest atoms are shaded.

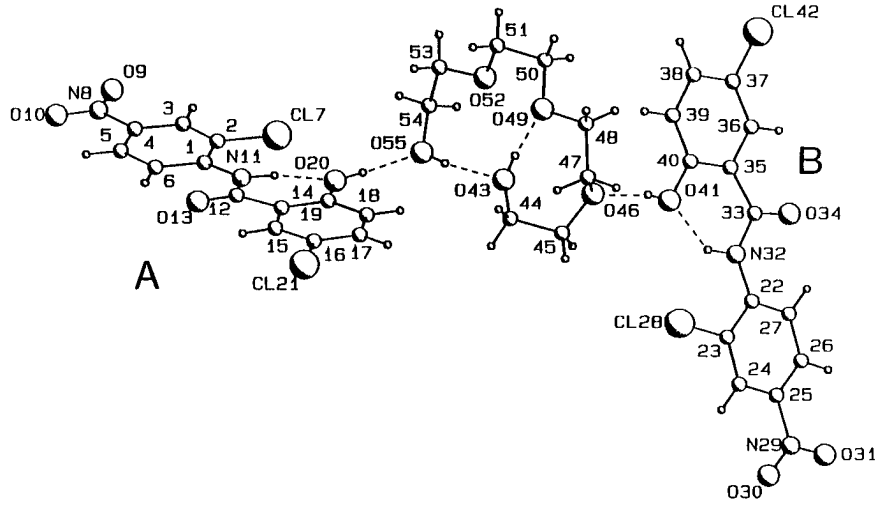

Figure 9. Conformations of the two independent host molecules and the TEG molecule in **3** showing principal hydrogen bonds. For clarity, C atoms are labelled with numerals only.

successive host layers contain, alternately, A and B molecules. Cohesion between a layer of guest molecules and adjacent host layers is effected by O—H· · ·O hydrogen bonds, namely those shown in detail in Figure 9, repeated by space group symmetry and lattice translation. Thermogravimetry indicated mass loss due to TEG liberation over a wide temperature range (65–230 °C) [7]. Spontaneous desolvation of crystals of **3** in the atmosphere at 20 °C is very slow. These observations are consistent with the low volatility of TEG (b.p. 328 °C) and with the fact that each TEG molecule

Table VI. Torsion angles (^{o}) for the tetraethylene glycol molecule in **3**.

O(43)—C(44)—C(45)—O(46)	53.4(4)
C(44)—C(45)—O(46)—C(47)	70.3(4)
C(45)—O(46)—C(47)—C(48)	−134.6(3)
O(46)—C(47)—C(48)—O(49)	66.3(4)
C(47)—C(48)—O(49)—C(50)	−160.2(3)
C(48)—O(49)—C(50)—C(51)	−173.0(3)
O(49)—C(50)—C(51)—O(52)	−59.2(4)
C(50)—C(51)—O(52)—C(53)	178.7(3)
C(51)—O(52)—C(53)—C(54)	−177.1(3)
O(52)—C(53)—C(54)—O(55)	67.7(5)

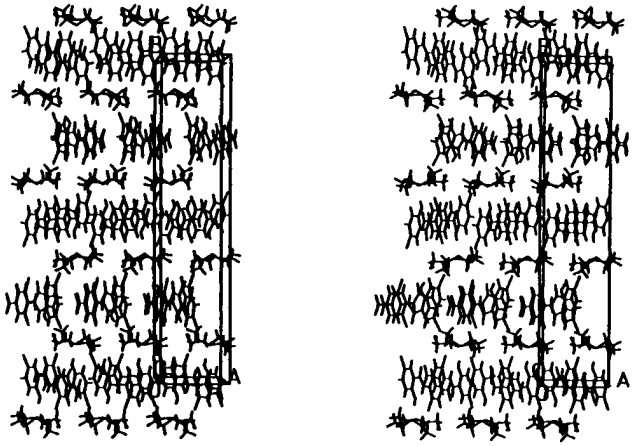

Figure 10. Stereodiagram of the crystal structure of **3**.

is very strongly bound by O—H· · ·O hydrogen bonds to both host layers between which it intercalates.

4. Conclusion

In the solid state, the preferred conformation of the niclosamide molecule in the pseudopolymorphs investigated is the β-form, as indicated by its occurrence in four independent instances. In this conformation, which is stabilised by intramolecular attractive interactions, the drug —OH function is free to recognise guest molecules containing O acceptor atoms and does so by O—H· · ·O hydrogen bonding. The topology of guest inclusion differs widely with the nature of the included solvent but is in each case consistent with the observed desolvation behaviour. The role of tetraethylene glycol as a guest in an inclusion compound has been demonstrated.

Acknowledgements

We thank the University of Cape Town and the Foundation for Research Development (Pretoria) for financial assistance.

References

1. T. Laird: in C. Hansch, P.G. Sammes, and J.B. Taylor (eds.), *Comprehensive Medicinal Chemistry* Vol. 1, p. 356, Pergamon Press, Oxford (1990).
2. M.R. Caira and R. Mohamed: *Supramol. Chem.* **2**, 201 (1993).
3. M.R. Caira, J.J. Gerber, and A.P. Lötter: *Supramol. Chem.* **5**. 225 (1995).
4. E. Weber, I. Csöregh, B. Stensland, and M. Czugler: *J. Am. Chem. Soc.* **106**, 3297 (1984).
5. R.S. Goldsmith: in B.G. Katzung (ed.), *Basic and Clinical Pharmacology*, pp. 659–660, Lange Medical Publications, California (1984).
6. *The Merck Index*, 11th Edn., S. Budavari (ed.), p. 1029, Merck & Co., New Jersey (1989).
7. E. C. van Tonder: *Preparation and Characterisation of Niclosamide Crystal Modifications*, Ph.D. thesis, Potchefstroom University for CHE, June 1996.
8. E.C. van Tonder, M.R. Caira, M.M. de Villiers, and A.P. Lötter: *Int. J. Pharm.* In preparation (1996).
9. G.M. Sheldrick: *Acta Crystallogr.* **A46**, 467 (1990).
10. G.M. Sheldrick: SHELX76, *A System of Computer Programs for X-ray Structure Determination*, Cambridge University, UK (1976).
11. G.H. Stout and L.H. Jensen: *X-ray Structure Determination, A Practical Guide*, p. 210, Macmillan, New York (1965).
12. M. Nardelli: *Comput. Chem.* **7**, 95 (1983).
13. W.D.S. Motherwell: PLUTO, *A Program for Plotting Molecular and Crystal Structures*, Cambridge University, UK (1979).
14. L.J. Barbour: *Clathration by Diol Hosts: Thermodynamics and Structure.* Ph.D. thesis, University of Cape Town, South Africa (1994).
15. L.I. Kosheleva and A.F. Bekhli: *Khim.-Farm. Zh.* **8**, 57 (1974).
16. M.R. Caira, L.R. Nassimbeni, M.L. Niven, W.-D. Schubert, E. Weber, and N. Dörpinghaus: *J. Chem. Soc. Perkin Trans 2*, 2129 (1990).
17. Cambridge Structural Database and Cambridge Structural Database System (Version 5.11), Cambridge Crystallographic Data Centre, University Chemical Laboratory, Cambridge, UK, April 1996.
18. *The Merck Index*, 11th Edn., S. Budavari (ed.), p. 1204, Merck & Co., New Jersey (1989).